

FDTD Simulation Bowtie Dipole Antenna to Detect Small Objects and Geometric Shape Regular and Irregular by GPR

Fouad Lahlal, Ahmed Faize, Mohamed Atounti and Gamil Alsharahi

Department of Physics, Faculty of Polydisciplinary, Mohammed First University, Oujda, Morocco

Key words: Ground Penetrating Radar (GPR), bowtie dipole antenna, simulation, ability, detection, objects

Corresponding Author:

Fouad Lahlal

Department of Physics, Faculty of Polydisciplinary, Mohammed First University, Oujda, Morocco

Page No.: 3399-3406

Volume: 15, Issue 19, 2020

ISSN: 1816-949x

Journal of Engineering and Applied Sciences

Copy Right: Medwell Publications

Abstract: This research aims to simulate the efficiency bowtie dipole antenna to detect buried objects and their suitability in many different situations and conditions by Ground Penetrating Radar (GPR). Also, among the objectives its ability to detection regular and random objects in a geometric shape. GPR technology is very important and it is used in many applications as (Civil engineering, geophysics, geology and other applications). One of the most important steps in the work of GPR radar is to choose the type of antenna used and its ability to detect small objects. In this research, we focused on a bowtie dipole antenna and we worked on many models by simulating using programs based on the FDTD method.

INTRODUCTION

In recent years, the Nondestructive Testing (NDT) of structures and soils using GPR has become a mature technology. The particular interest in this technique is explained by several advantages when compared to other NDT techniques: the portability of the equipment because of its moderate weight, relatively low cost of the survey, the reasonable budget of the initial investment and high versatility in terms of application for different purposes and scenarios. However, the success of GPR surveys is not straightforward due to the complexity of the physical phenomena involved^[1-2].

The applicability of GPR as an aid to monitoring these processes has been investigated. GPR surveys have successfully resolved the shallow depth soil and geological structure^[3-5].

This study aims to present the initial results obtained in the first phase of a long-term effort to build a numerical model of the GPR operation on Mars and test dedicated signal processing algorithms on the simulated data. The simulation is based on the use of a Finite Difference Time

Domain method (FDTD) and we have pointed out some of its advantages that allow us to take into account the complex features of the underground. FDTD method is used to analyze a practical GPR antenna system operating above lossy and dispersive grounds. The antenna is of the resistor-loaded bow-tie type and the analysis is made for two known soil types, namely Puerto Rico and San Antonio clay loams^[6-9].

GPR is a high-resolution geophysical method which is based on the propagation of high-frequency electromagnetic waves. Three decades, since, the commercialization of GPR, the vast majority of radar instruments are now applied for civil infrastructure applications. GPR is a surface-geophysical method that depends on the emission, transmission, reflection and reception of an electromagnetic pulse and can produce continuous high-resolution profiles of the subsurface rapidly and efficiently^[10, 11]. The development of imaging to estimate the electromagnetic properties of the medium include the dielectric permittivity ϵ (F/m) and the electrical conductivity σ (S/m) which are critical issues for a physical interpretation of the target structures.

Moreover, GPR is based on the transmission and reception of 10-2.6 GHz electromagnetic waves into the ground^[12, 13]. The quantitative characterization of the shallow subsurface of the Earth is a critical issue for many environmental and societal challenges. GPR is a geophysical method based on the propagation of electromagnetic waves for the prospection of the near subsurface. GPR covers a wide range of applications in geology, hydrology and civil engineering^[14].

GprMax2D was also used with the development of the code and improved to achieve the goal of this work. We have obtained satisfactory and useful results through which we can determine the type of objects as conductors or dielectrics and also the geometric shape of these objects^[15].

MATERIALS AND METHODS

Description method and software

FDTD based on GPR modelling and simulation: Maxwell's electromagnetic equations that mathematically express the relations between the fundamental electromagnetic field quantities and their dependence on their sources can be used to describe all electromagnetic phenomena. The fundamental equations are acquisition methods that have to be synchronized and all referred to the same coordinate system to integrate the geometric data collected by the different techniques^[16, 17]. There are four basic equations, called Maxwell equations which form the axioms of electromagnetic, these equations are the following:

$$\text{rot } \underline{H} = \underline{j} + \partial \underline{D} / \partial t \quad (1)$$

$$\text{rot } \underline{E} = -\partial \underline{B} / \partial t \quad (2)$$

$$\text{div } \underline{B} = 0 \quad (3)$$

$$\text{div } \underline{D} = \rho \quad (4)$$

Where:

- \underline{H} = Vector of the magnetic field strength
- \underline{j} = The current density vector
- $\partial \underline{D}$ = The time derivative of the electric displacement vector \underline{D}
- \underline{E} = The electric field strength
- $\partial \underline{B} / \partial t$ = The time derivative of the magnetic induction a vector
- \underline{B} = div is the so-called source density
- ρ = The charge density

The ultimate objective of the work which has been undertaken is to build a numerical code that can simulate with enough accuracy the operation of the GPR in an actual environment in order to evaluate the real performances of the GPR. We have selected the FDTD

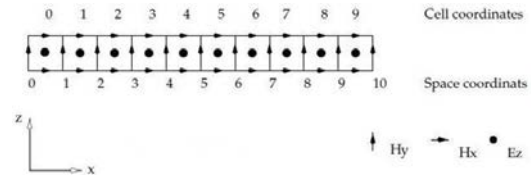


Fig. 1: The two-dimensional FDTD cell

method to describe the wave propagation and electromagnetic coupling of the antenna with the soil.

System of GPRMax2D: The “GprMax 2/3D” is a program designed in 1996 by Antonios Giannopoulos, University of York Island. Aim to a wave simulator 2D and 3D of GPR as required by using the best adapted version of the desired work. It is based on the numerical method the FDTD^[18, 19].

The GprMax 2D FDTD algorithm is implemented in the plane (x-y) where the origin of the coordinate system is the lower left corner at (0, 0). The smallest space that can be allocated to represent a specific medium is a 2D cell ($\Delta x \times \Delta y$) with the reference point at its center. The space coordinates however range from the left edge of the first cell to the right edge of the last one as depicted in Fig. 1. For a given set of space coordinates (x, y), the actual positions of the EM field components are^[19]:

$$\left(x + \frac{\Delta x}{2}, y + \frac{\Delta y}{2} \right) \text{ for } E_z$$

$$\left(x + \frac{\Delta x}{2}, y \right) \text{ for } H_x$$

$$\left(x, y + \frac{\Delta y}{2} \right) \text{ for } H_y$$

which are due to the staggered arrangement of field components in the FDTD algorithm. Therefore, the interference between two cells of different constitutive parameters is located on the positions of the magnetic field components and all sources are actually located at the positions of the E_z field component^[19].

Principle of GPR: Electrode magnetic the waves emitted into the ground and time measured for wave to be reflected and received (Fig. 2). When wave hits areas of change in soil, it is hit back to receiver antenna changes in soil can include objects buried underneath the surface. Depth of Investigation varies from less than a meter to over 1000 m, depending upon material properties. Detectability of a subsurface feature depends upon contrast in electrical and magnetic properties and the

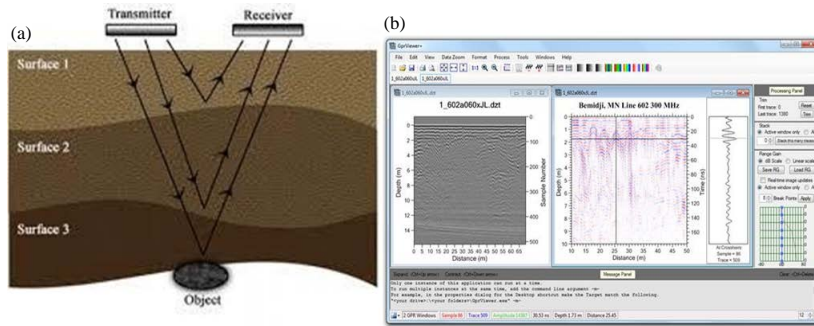


Fig. 2(a, b): General working principle of GPR

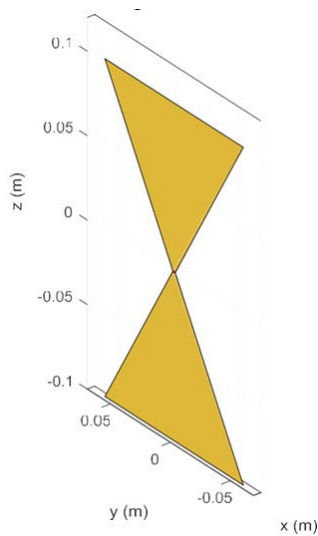


Fig. 3: The basic geometry of a typical triangular bowtie antenna

geometric relationship with the antenna. Quantitative interpretation through modeling can derive from GPR data such information as depth, orientation, size and shape of buried objects, density and water content of soils and much more. For homogeneous isotropic materials, the relative propagation speed v_r can be defined by (Fig. 3):

$$v_r = \frac{c}{\sqrt{\epsilon_r}} \text{ (m/s)} \quad (5)$$

And the depth can be calculated by:

$$d = v_r \frac{t_r}{2} \text{ (m)} \quad (6)$$

Where:

ϵ_r = The relative permittivity

t_r = The time of sending and receiving

Bowtie antenna: Bow tie antennas are the most widely used in GPR due to their wide impedance matching and radiation properties. The bow-tie antenna has a dipole type diagram and the wave emitted by this antenna is linearly polarized. The typical gain of the bow-tie antenna is 5-6 dBi which is higher than normal dipole antennas. In addition, it can operate on a wider frequency band compared to dipole antennas or dipole antenna with a resistive load^[20].

- Frequency (MHz): 400; Wavelength (mm): 749.5
- Bandwidth (MHz): 132; Distance (mm): 15.5
- Width (mm): 281.1; Height (mm): 187.4

RESULTS AND DISCUSSION

To simulate the GPR signals of objects by GprMax2d, we need a certain number of parameters such as the frequency of the antenna used, the geometry of the subsoil and targets, the dielectric permittivity, the magnetic permeability and the electrical conductivity. On a GPR image, each object below the surface appears as a hyperbola due to repeated reflections produced as the GPR unit passes over an object. In what follows, the results obtained for the different simulations carried out for different material as Table 1.

Buried targets in medium homogeneous: The model of simulation by GprMax2d for detection of the buried objects in soil whose characteristics ($\epsilon_r = 8$ and $s = 0.0001$ S/m) and along 2 m, depth 1 m (Fig. 4). Buried objects are empty and iron of various shapes ($\epsilon_r = 1$ and $s = 0$ for empty and $\epsilon_r = 1$ and $s = 1010$ S/m) at a depth of 0.5 m (Fig. 4ab).

Figure 4c and 4d present the radargram of detection the objects shown by hyperbolas and Fig. 3e and 3f show the trace of reflection signal from the surface the objects. Notice in Fig. 4a, the first object in the form of a triangle, the second body is rectangular, the third in the form of a semicircle and the fourth as a circle. Through these forms,

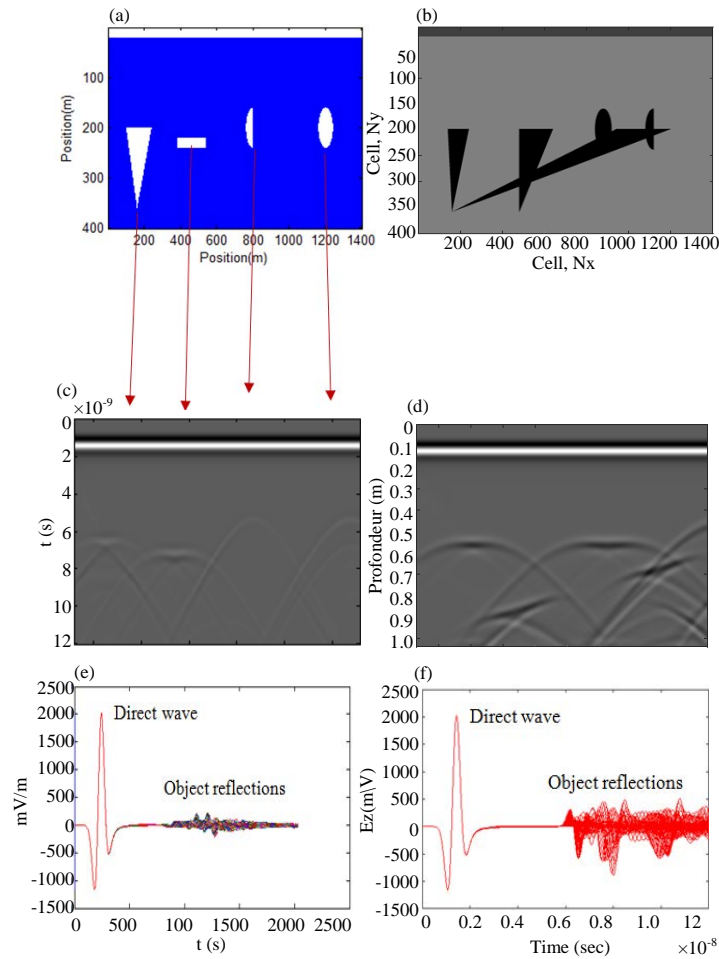


Fig. 4(a-f): Model of detection the empty and iron at $f = 400$ MHz (a, b) Modelling by GprMax2d (c, d) Radargrams of detect targets (e, f) Simulation GPR trace

the difference in the hyperbola (Fig. 4c) of the reflected signals from the surface of each object. In Figure 4b, we notice the presence of overlapping and irregular shapes as well. Here, there is a difference in the shape of the hyperbola (Fig. 4d) and that the radar's ability to identify and distinguish those buried objects is high.

In Fig. 5, we show a model to detect different circular objects (water, plastic, water sea, iron and empty) buried in the middle of the soil (Fig. 5a). Figure 5b presents the radargram of detection the objects as shown by hyperbolas and Fig. 5c shows the race of reflection signal from the surface the objects.

In Fig. 6, very small circular ($R = 0.05$) objects (concrete, iron, empty, rock) will be buried at depth 1m in a medium of soil as Fig. 6a ($O_x 3m$ and $O_y 2m$) and GPR performance will be tested in detecting it and determining its depth. Figure 6b represents a radargram detection of buried objects and determine their depth through the

Table 1: Properties physical of materials used in simulation

| Materials | Relative permittivity | Conductivity (s/m) | Velocity (m/ns) |
|-----------|-----------------------|--------------------|-----------------|
| wood | 3 | 0.003 | 0.170 |
| Iron | 1.45 | 9.99×10^6 | 0.240 |
| Empty | 1 | 0 | 0.300 |
| Dry sand | 3 | 0.0001 | 0.170 |
| Water | 81 | 0.0005 | 0.030 |
| Sea water | 81 | 0.5-4 | 0.030 |
| Plastic | 4 | 0.002 | 0.150 |
| Rock | 10 | 0.1 | 0.090 |
| Brick | 4 | 0.001 | 0.150 |
| Clay wet | 20 | 0.1 | 0.067 |

appearance of the hyperbola. Figure 6c trace GPR signal. In Fig. 7, GPR radar performance will be tested to detect and distinguish two crossed objects buried in the medium of soil. Figure 7b represents a radargram detection of buried objects and determine their depth through the appearance of the hyperbola. Figure 7c trace GPR signal.

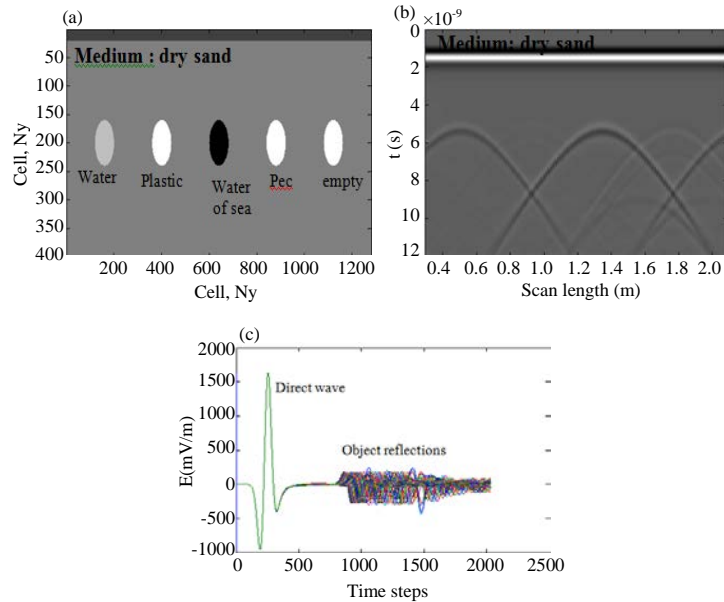


Fig. 5(a-c): Model of detection different circular objects at $f = 400$ MHz, (a) Modelling by GprMax2d, (b) Radargram of model detect medium contain targets and (c) Simulation GPR trace

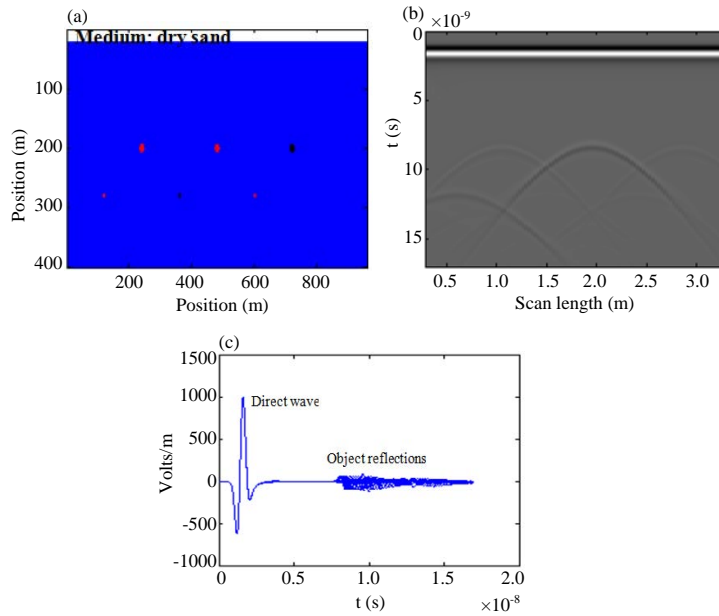


Fig. 6 (a-c): Model of soil contain small targets at $f = 400$ MHz, (a) Modelling by GprMax2d, (b) Radargram of model detect medium contain small targets and (c) Simulation GPR trace

Buried targets in medium (layer and targets): The study environment this time consists of layers and the geometric models of the objects to be simulated in this medium are shown in Fig. 8 and 9.

In this part, we test GPR as a tool for detecting layers and targets together in the soil. Several GPR transects

were established in soil (Fig. 8 and 9). In Fig. 7a we have a group of layers and buried objects as Fig. 8a. Figure 8b and 9b represents a radargram detection of buried objects and layers through the appearance of the hyperbola. Figure 8c and 9c trace the GPR signal.

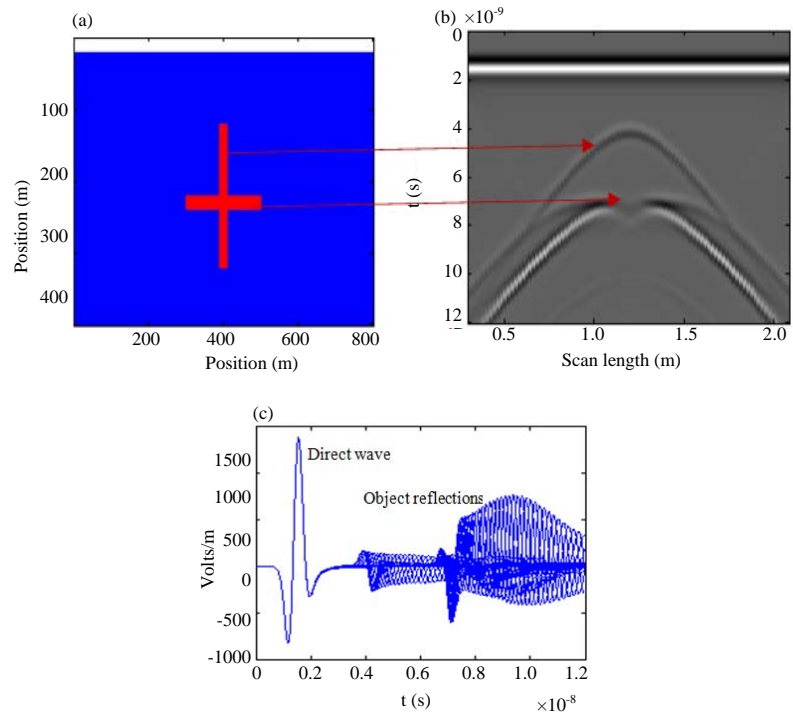


Fig. 7(a-c): Model of soil contain two targets at $f = 400$ MHz, (a) Modelling by GprMax2d, (b) Radargram of model detect two targets and (c) Simulation GPR trace

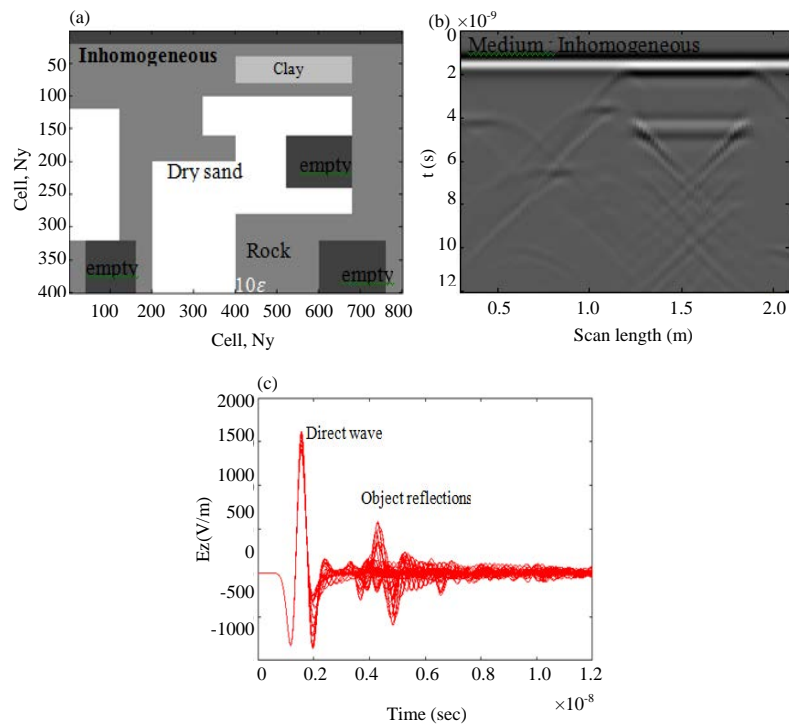


Fig. 8(a-c): Model of soil (geological) at $f = 400$ MHz, (a) Modelling by GprMax, (b) Radargram of detect layer and targets and (c) Simulation GPR trace

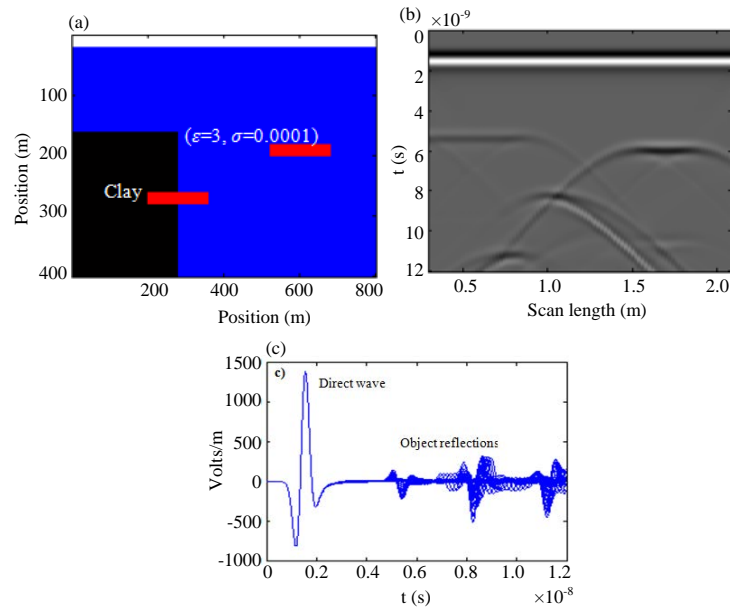


Fig. 9(a-c): Model of soil and $f = 400\text{MHz}$, (a) Modelling by GprMax2d, (b) Radargram of detect layer and targets and (c) Simulation GPR trace

CONCLUSION

The simulation of the signals taken by the GPR radar and ability by the software GprMax2d were successful. The simulations, we carried out relate to dielectric and conductive objects in different shapes and volumes. In all the radargrams images, simulated or obtained, one notices the presence of the indicator hyperbolas which gives information on the buried underground objects (depth, position according to the spatial directions x and y). We notice from the figures that hyperbola differs depending on the geometrical shape of the buried object and also on the physical properties of the object. Through the results obtained, the GPR ability to detect small objects buried in various conditions was very large.

REFERENCES

01. Ida, N. and N. Meyendorf, 2019. Handbook of Advanced Non-Destructive Evaluation. Springer, Berlin, Germany, Pages: 1626.
02. Daniels, D.J., 2004. Ground Penetrating Radar. 2nd Edn., The Institution of Electrical Engineers, London, UK..
03. Huici, M.G., 2013. Accurate ground penetrating radar numerical modeling for automatic detection and recognition of antipersonnel landmines. Ph.D. Thesis, Universit ats-und Landesbibliothek Bonn, Bonn, Germany.
04. Ciarletti, V., B. Martinat, A. Reineix, J.J. Berthelie and R. Ney, 2003. Numerical simulation of the operation of the GPR experiment on Netlander. *J. Geophys. Res. Planets*, Vol. 108, 10.1029/2002JE001867
05. Taflove, A. and S.C. Hagness, 1995. Computational Electromagnetics: The Finite-Difference Time-Domain Method. In: *The Electrical Engineering Handbook*, Wai-Kai, C. (Eds.), Elsevier Academic Press, Boston, Massachusetts, pp: 149-161.
06. Goodman, D., 1994. Ground-penetrating radar simulation in engineering and archaeology. *Geophys.*, 59: 224-232.
07. Gurel, L. and U. Oguz, 2001. Simulations of ground-penetrating radars over lossy and heterogeneous grounds. *IEEE. Trans. Geosci. Remote Sens.*, 39: 1190-1197.
08. Uduwawala, D., M. Norgren, P. Fuks and A. Gunawardena, 2005. A complete FDTD simulation of a real GPR antenna system operating above lossy and dispersive grounds. *Progress Electromagn. Res.*, 50: 209-229.
09. Rappaport, C. and M. El-Shenawee, 2000. Modeling GPR signal degradation from random rough ground surface. *Proceedings of the IGARSS 2000 IEEE 2000 International Geoscience and Remote Sensing Symposium on Taking the Pulse of the Planet: The Role of Remote Sensing in Managing the Environment (Cat. No. 00CH37120) Vol. 7, July 24-28, 2000, IEEE, Honolulu, Hawaii, pp: 3108-3110.*

10. Davis, J.L. and A.P. Annan, 1989. Ground-Penetrating Radar for high-resolution mapping of soil and rock stratigraphy. *Geophys. Prospect.*, 37: 531-551.
11. Beres Jr, M. and F.P. Haeni, 1991. Application of ground-penetrating-radar methods in hydrogeologie studies. *Groundwater*, 29: 375-386.
12. Alsharahi, G., M.M.A. Mint, A. Faize and A. Driouach, 2016. Modelling and simulation resolution of ground-penetrating radar antennas. *J. Electromagn. Eng. Sci.*, 16: 182-190.
13. Alsharahi, G., A. Faize, M. Louzazni, A.M.M. Mostapha and M. Bayjja *et al.*, 2019c. Detection of cavities and fragile areas by numerical methods and GPR application. *J. Appl. Geophys.*, 164: 225-236.
14. Lavoue, F., R. Brossier, S. Garambois, J. Virieux and L. Metivier, 2015. 2D full waveform inversion of GPR surface data: permittivity and conductivity imaging. *Proceedings of the 2013 7th International Workshop on Advanced Ground Penetrating Radar*, July 2-5, 2015, IEEE, Nantes, France, pp: 1-6.
15. Alsharahi, G., A. Faize and A. Driouach, 2019a. Determination of the physical properties and geometric shape of objects buried by simulation signals radar GPR. *Proceedings of the 2019 8th International Conference on Modeling Simulation and Applied Optimization (ICMSAO)*, April 15-17, 2019, IEEE, Manama, Bahrain, pp: 1-4.
16. Alsharahi, G., A. Faize, C. Maftai, M. Bayjja, M. Louzazni, A. Driouach and A. Khamlichi, 2019b. Analysis and modeling of GPR signals to detect cavities: Case studies in Morocco. *J. Electromagn. Eng. Sci.*, 19: 177-187.
17. Zhang, Z. and S. Satpathy, 1990. Electromagnetic wave propagation in periodic structures bloch wave solution of Maxwells equation. *Physical Rev. Lett.*, 65: 2650-2653.
18. Giannopoulos, A. and N. Diamanti, 2008. Numerical modelling of ground-penetrating radar response from rough subsurface interfaces. *Near Surf. Geophys.*, 6: 357-369.
19. Warren, C., A. Giannopoulos and I. Giannakis, 2016. gprMax: Open source software to simulate electromagnetic wave propagation for ground penetrating radar. *Comput. Phys. Commun.*, 209: 163-170.
20. Turk, A.S., D.A. Sahinkaya, M. Sezgin and H. Nazli, 2007. Investigation of convenient antenna designs for ultra-wide band GPR systems. *Proceedings of the 2007 4th International Workshop on Advanced Ground Penetrating Radar*, June 27-29, 2007, IEEE, Naples, Italy, pp: 192-196.